2013

IMPROVED SYNTHESIS OF 3-ARYL-ISOXAZOLES AS INTERMEDIATES FOR NOVEL G-QUADRUPLEX BINDING ANTI-TUMOR AGENTS

Matthew Jacob Weaver
The University of Montana

IMPROVED SYNTHESIS OF 3-ARYL-ISOXAZOLES AS INTERMEDIATES FOR NOVEL G-QUADRUPLEX BINDING ANTI-TUMOR AGENTS

By

MATTHEW JACOB WEAVER

B.S. in Biological Chemistry, The University of Montana, Missoula, MT, 2011

Thesis

presented in partial fulfillment of the requirements
for the degree of

Master of Science
in Medicinal Chemistry

The University of Montana
Missoula, MT

July 2013

Approved by:

Sandy Ross, Dean of The Graduate School
Graduate School

Nicholas R. Natale, Medicinal Chemistry Graduate Program Chair
Biomedical and Pharmaceutical Sciences

Howard D. Beall, Vice-Chair of the Department of Biomedical and Pharmaceutical Sciences

Kent D. Sugden
Department of Chemistry

COPYRIGHT NOTICE TEMPLATE
(This page is not required. For legal purposes, full name of author must be used. This page is not required. There is a $45 fee for students wanting to register their copyright through UMI. Delete these instructions.)

Weaver, Matthew, M.S., Summer 2013 Medicinal Chemistry

Improved synthesis of 3-aryl-isoxazoles as intermediates for novel G-quadruplex binding anti-tumor agents

Nicholas R. Natale

As a promising new target for chemotherapy G-quadruplexes (G4) have drawn great interest from the scientific community. Current chemotherapeutic agents exhibit broad toxicity to patients; G4 has the potential to be selectively targeted by novel chemotherapeutic agents that exhibit toxicity specific towards cancer cells. Anthracenyl isoxazolyl amides (AIMs) have shown potent anti-tumor activity and have evidence to support them as G4 binding molecules. Studies of the AIMs' unique mechanism of action require an efficient synthesis of target molecules. For our system, methods traditionally used to synthesize isoxazoles were inefficient and gave poor yields. A critical comparison of methods to prepare sterically hindered 3-aryl isoxazoles containing fused aromatic rings using the nitrile oxide cycloaddition (NOC) revealed that modification of the method of Bode, Hachisu, Matsuura and Suzuki (BHMS), was far superior to that of the enamine method. Utilization of either triethyl amine as a base or sodium enolates of diketone, ketoester and ketoamide dipolarophiles gave much higher yields as well as fewer by-products from the NOC. Here-in is reported the improved synthesis of 3-aryl-isoxazoles via an adaption of the BHMS method. Included in this report is the crystallographic data for Ethyl 3-(10'-bromo-9'-anthracenyl)-5-methyl-4-isoxazolcarboxylate. As seen in the crystal structure of the chapter 2 title compound the isoxazole plane is nearly orthogonal to the plane of the anthracene; which is thought to be a necessity for the AIMs to interact with G4. This conformation is ideal for both pi-stacking with the guanine decks and polar interactions with the phosphate backbone of quadruplex DNA.

Table of Contents

Acknowledgments

This work would not have been possible without the support of my family, friends, and colleagues. I would like to thank Dr. Natale for initiating and facilitating my ever growing interest in medicinal chemistry. I must also acknowledge and thank my parents for teaching me, by example, the meaning of hard work and how to implement work ethic into one's life as well as a career.

List of Figures

Introduction

There are many cellular mechanisms by which a cell attempts to maintain the crucial balance between proliferation and apoptosis. When these mechanisms fail the cell either dies or goes into uncontrolled proliferation which is considered one of the "hallmarks of cancer" (Hanahan and Weinberg, 2011). This immortality may be achieved by circumventing the natural aging mechanisms. Maintenance of telomeres by telomerase plays a crucial role in a cells ability to replicate indefinitely (Kelland, 2007). Small molecules that could recognize and bind the telomere would have the potential inhibit cancer growth by blocking telomerase from replicating the telomere. One target that may allow for small molecules to select for telomeric DNA is the G-quadruplex (G4) (Burge, *et al*., 2006).

Human DNA can adopt many structures other than that of the classical double-helix. G-quartets are planar structures formed in guanine-rich regions of DNA and RNA. These quartets often stack in sets of three and have been shown to form several three-dimensional G4 structures in isolated DNA sequences (Neidle, 2012). The presence of G4 has also been recently quantified in human cells (Biffi, et al., 2013). Telomeric G4 has drawn considerable interest as maintenance of the telomere is essential for proliferation among cancer cells (Neidle, 2000). Proof-of-concept was achieved as quarfloxin, a first in class quadruplex binding small molecule, reached clinical trials (Balasubramanian, *et al*. 2011).

Anthracenyl isoxazole amides (AIMs), developed in our laboratory, have shown potent anti-tumor activity which does not correlate to a traditional mechanism of action (Han, *et al*, 2009). Using computational studies and DNA binding assays we plan to test

our hypothesis of AIMs as G4 binders. This hypothesis is backed by preliminary studies that suggest AIMs have the potential to interact with G4. In order for these studies to advance a more efficient synthesis of intermediates is required

References

Balasubramanian, S.; Hurley, L.H.; Neidle, S. Targeting G-quadruplexes in gene promoters: a novel anticancer strategy? *Nature Rev. Drug Discovery*, **2011**, *10*, 261-275.

Biffi, G.; Tannahill, D.; McCafferty, J.; Balasubamanian, B. Quantitative visualization of DNA G-quadruplex structures in human cells. Nature Chemistry, **2013**, 05, 182-186

Burge S, Parkinson GN, Hazel P, Todd AK, Neidle S. Quadruplex DNA: sequence, topology and structure. *Nucleic Acids Res*. **2006**, 34(19): 5402-15. PMCID: 1636468.

Han X, Li C, Mosher MD, Rider KC, Zhou P, Crawford RL, Fusco, W.; Natale, N.R. Design, synthesis and biological evaluation of a novel class of anticancer agents: anthracenylisoxazole lexitropsin conjugates. *Bioorg Med Chem*. **2009**;17(4):1671-80. PMCID: 2978248.

Hanahan D, Weinberg RA. Hallmarks of cancer: the next generation. *Cell*. **2011**;144(5):646-74.

Kelland L. Targeting the limitless replicative potential of cancer: the telomerase/telomere pathway. *Clin Cancer Res*. **2007**;13(17):4960-3.

Neidle, S. Targeting the end of DNA. *Chem. Brit*., **2000,** *36*, 27-29

Therapeutic Applications of Quadruplex Nucleic Acids, Stephen Neidle, Elsevier/Academic Press, Amsterdam, 2012.

Chapter 1: Improved synthesis of 3-aryl isoxazoles containing fused aromatic rings

Yousef R. Mirzaei, Matthew J. Weaver, Scott A. Steiger, Alison K. Kearns, Mariusz P. Gajewski, Kevin C. Rider, Howard D. Beall, and N.R. Natale*

Medicinal Chemistry Graduate Program

Department of Biomedical and Pharmaceutical Sciences

The University of Montana, Missoula MT 59812

This manuscript has been peer reviewed, and published in the journal *Tetrahedron*, **2012**, 68, 10360–10364.

Abstract— A critical comparison of methods to prepare sterically hindered 3-aryl isoxazoles containing fused aromatic rings using the nitrile oxide cycloaddition (NOC) reveal that modification of the method of Bode, Hachisu, Matsuura and Suzuki (BHMS), utilizing either triethyl amine as base or sodium enolates of the diketone, ketoester and ketoamide dipolarophiles, respectively was the method of choice for this transformation.

Introduction

Isoxazoles continue to be of interest for both their biological activities and synthetic utility.[1-4] The synthesis of aryl-isoxazoles is also the subject of on-going improvements.[1,5-7] In connection with our studies on aryl isoxazole amides (AIMs)[8-9] we have reported lead compounds which possess (1) useful antitumor activity and (2) photophysical properties which are of potential diagnostic use as "tumor paint".[10]

An illustration of the application of AIMs is shown in **Fig. 1.** AIM NSC 728558 has exhibited a mid-graph mean point of -5.71-5.75 (log scale, which translate to single digit micromolar) for tumor cell line growth inhibition (GI_{50}) against the full panel in the NCI60 cell line antitumor screening protocol,[8] and as a benchmark for comparison clinically used agents 5-fluorodeoxyuridine, bleomycin and rubidazone gave values of -4.7, -5.2 and -5.8 respectively in the same standard assay. The calculated physical property data for NSC 728558 fall within or close to values with useful bioavailability (radar graph, Symyx Draw v3.1; top right panel). Laser Scanning Cytometry shows that NSC 728558 does in fact permeate human glioma SNB-19 cells (the AIM is blue) and is localized within the nucleus. Surgical resection of many cancers, especially brain tumors or gliomas, have a poor success rate because of the difficulty of judging the border between cancerous and healthy tissue. Fluorescent agents with antitumor activity such as the AIMs hold promise for improvements in visualizing tumors during surgery.[10b,c]

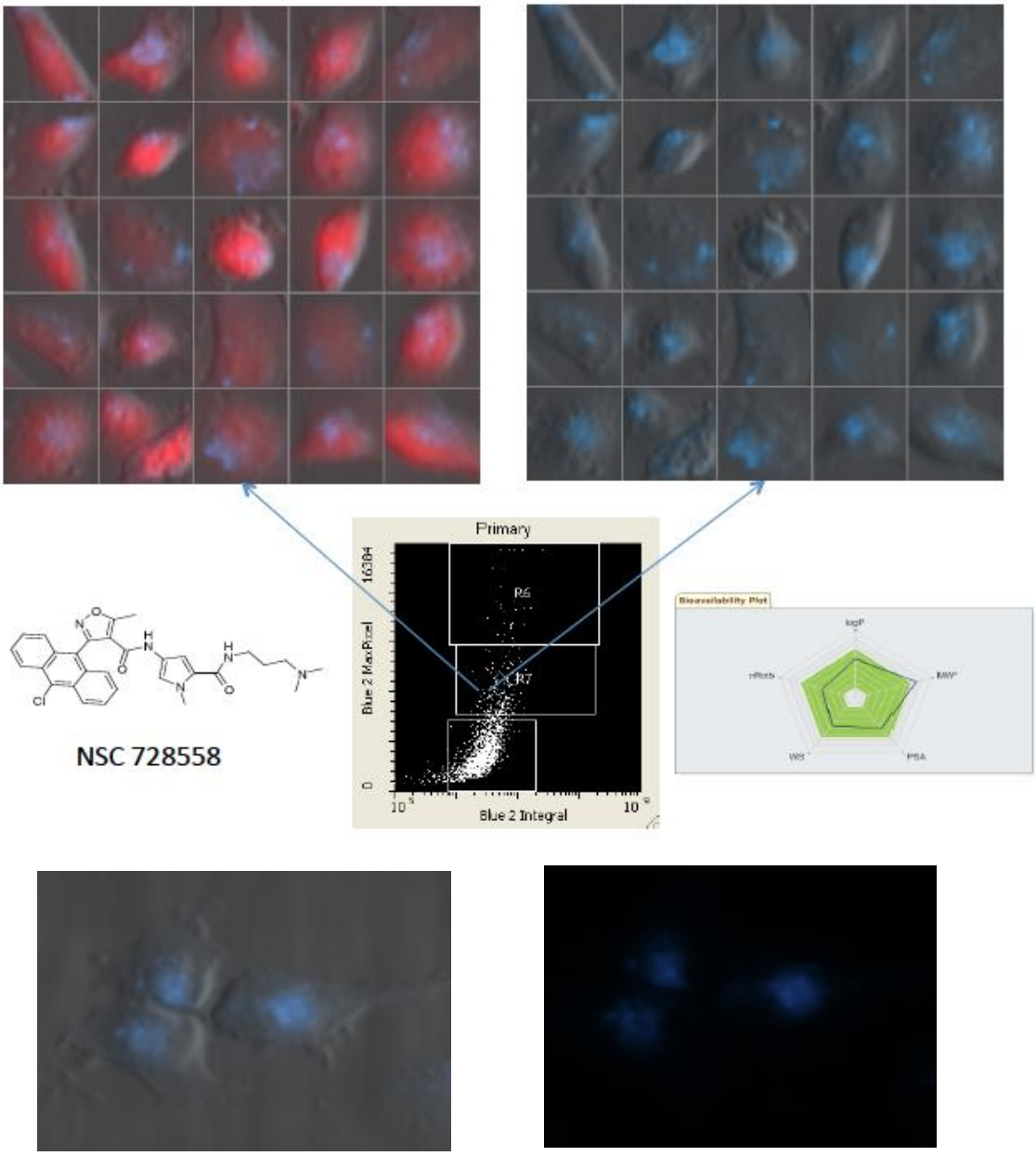

Fig. 1-1. Structure, Smyx radar graph, and Laser Scanning Cytometry of NSC 728558

We required both improvements in the efficiency of the preparation of the isoxazole *and* concomitant economy of scale to prepare amounts of material sufficient to expand the scope of our investigations toward *in vivo* studies.

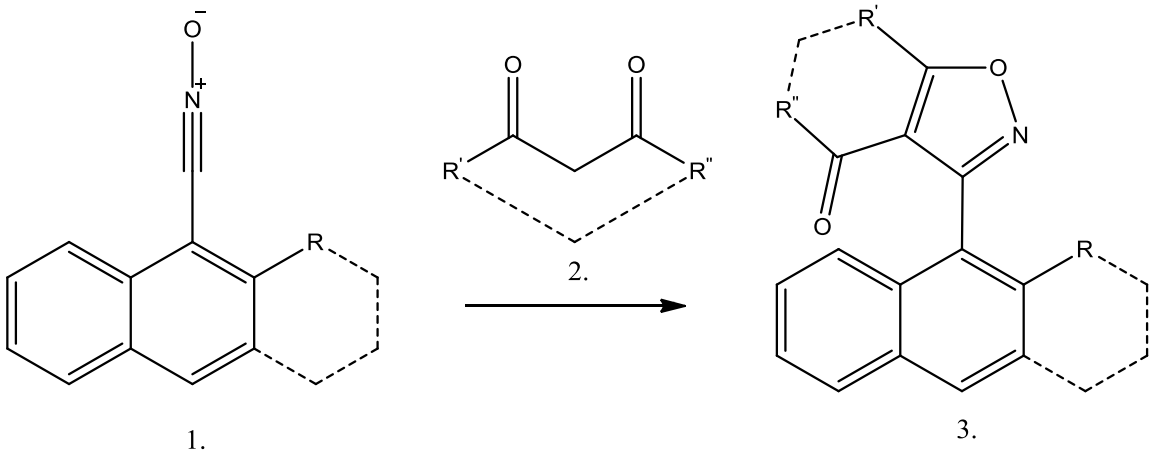

Chart 1-1. 1,3-dipolar cycloaddition

Isoxazoles prepared via nitrile oxide cycloaddition (NOC)[11] are most often prepared by dehydration of a-methylene nitro precursors,[5] or chlorination/dehalogenation of oximes[1,6,7] to form the nitrile oxide **1**.

Among the unsymmetrical dipolarophiles **2** which usually give rise to regioselective cycloaddition are enamines. First pioneered by Stork and McMurry,[12] the use of enamines in the NOC works well for aliphatic and aromatic nitrile oxides on mole scales.[1] We have employed modifications of this synthesis in the preparation of isoxazole-oxazolines,[13] antihypertensive 4-isoxazolyl-1,4-dihydropyridines,[14] and we have championed the reaction as a learning tool for aspiring chemists.[15] Our previous reports in the AIM series have used enamines as dipolarophiles,[16] while for most cases modest yields in the range of 30-40% overall of **3** were obtained, sufficient quantities of material were isolated for pharmacology studies. Upon scale-up however, we have observed a consistent diseconomy of scale using enamines and nitrile oxides derived

from fused ring aromatics, to the extent that even a ten-fold increase in scale (from *ca*. 10 to 100 mM) produced only marginally more desired product, and purified yields plummeted to 10-20%. *We have found this is especially a limitation when using nitrile oxides derived from fused aromatic systems*. Careful examination of the reaction by-products after chromatographic isolation and characterization by LC-MS revealed that as the stability of aryl nitrile oxides **1** increases[17,16b] their consequent reactivity to dipolarophiles slows, with concomitant increases in amine trapping of the nitrile oxide/oximidoyl chloride to give **7**, as well as self-condensation of the nitrile oxide to yield **8** as shown in **Scheme 1**.

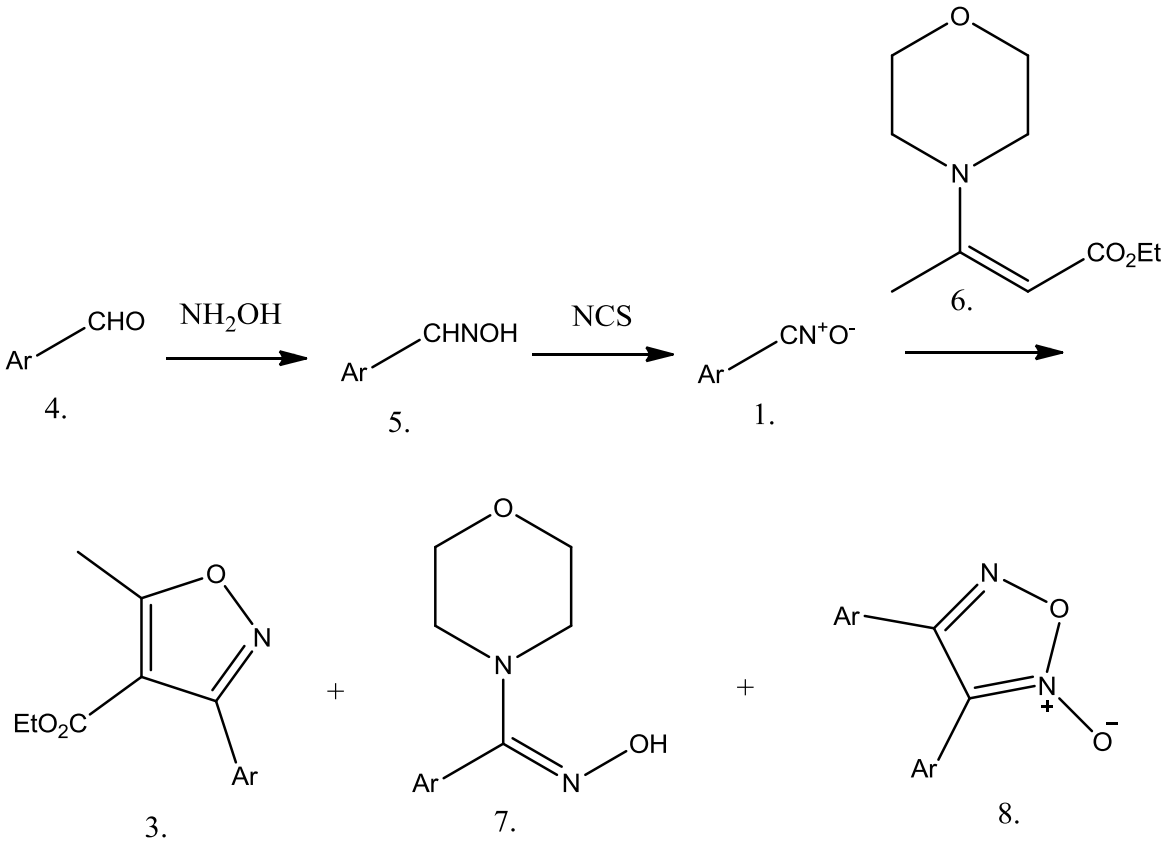

3b. Ar = 2-Me-Naphthyl 30-40% 7b. 46% 8b. 14%
3g. Ar = 2-MeO-Naphthyl 35% 7g. N/A 8g. 6%
3k. Ar = 10-Cl-Anthr-9-l 10-20% 7k. 29% 8k. N/A

Scheme 1-1. Synthesis of the isoxazoles used for the present study.

We therefore examined the methodology of Bode, Hachisu, Matsuura and Suzuki (BHMS), which use either the sodium enolates of ketoesters,[6] or tertiary amines as base.[7] The use of sodium enolates in the NOC was pioneered by Renzi and Dal Piaz,[20] and recently applied in 2,6-disubstituted aryl cases for the preparation of growth hormone secretagogue receptor antagonists.[21] The BHMS procedure has been used to prepare particularly hindered unsymmetrical 2,6-disubstituted aryl examples, including examples which appear to exist as atropisomers,[7] which recommended its application to our examples.

Using the BHMS procedure, the yields in all cases where critical comparison was made were dramatically improved (**Table 1**). Symmetrical diketones (**Table 1**, Entries 1, 4, 5 and 11-13), unsymmetrical arylalkyl ketones (**Table 1**, Entries 3, 9 and 10) and ketoesters (**Table 1**, Entries 2, and 6-8) all produced the desired isoxazole products. In particularly hindered situations the triethyl amide protocol[7] often gave higher yields than the sodium ethoxide method.[6] (**Table 1**, Entries 1, 3, 4 and 7, and compare entry 10 to 9), although in a select few cases we have observed that sodium isopropoxide to produce slightly higher yield (exemplified by **Table 1**, Entries 11 and 14). All of the BHMS methods gave superior results to our experience using enamines as dipolarophiles for fused 3-aryl isoxazoles: for **3b** the BHMS conditions gave 70% (**Table 1**, Entry 2) yield compared to 30-40% for the enamine method for which the by-products complicated purification and lowered the yield of desired isoxazole (**Scheme 1**). Similar results were observed for **3g** the yields were 80% (**Table 1**, Entry 8) for the BHMS versus 35% for enamine (**Scheme 1**). In cases where the BHMS yields are modest, the enamine

methodology gave only traces or no desired product at all that is, the enamine entries (not shown) corresponding to **Table 1**, Entries 3 9,and 10, would correspond to traces at best).

Table 1-1. Nitrile oxide cycloaddition synthesis of hindered 3-naphthyl-isoxazoles

Entry	Nitrile Oxide	Dipolarophile	Conditions	Product	Yield %
1	1a	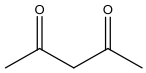	Et_3N	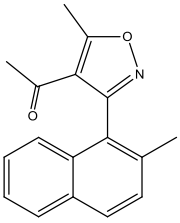 3a	40
2	1a	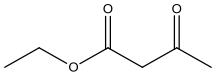	Na/EtOH	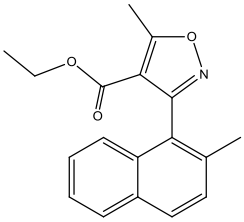 3b	70
3	1a	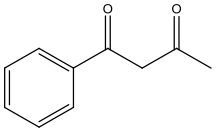	Et_3N	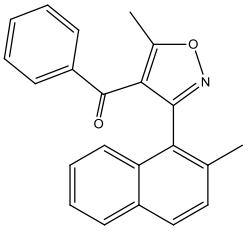 3c	40
4	1a	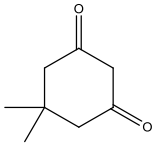	Et_3N	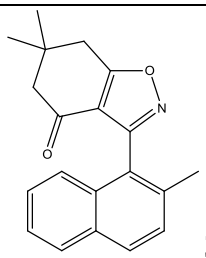 3d	71

5	1b	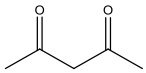	Na/EtOH	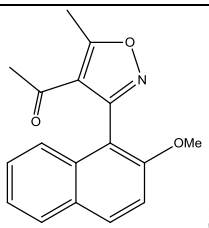 3e	70
6	1b	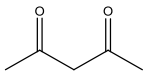	Et_3N	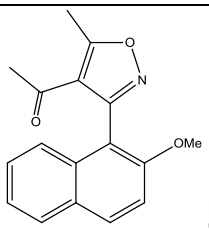 3e	67
7	1b	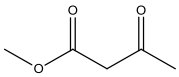	Na/EtOH	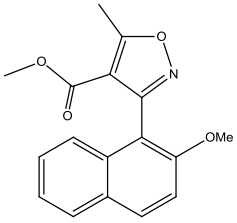 3f	60
8	1b	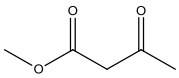	Et_3N	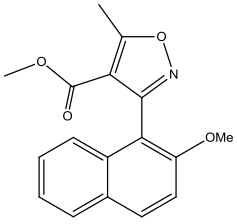 3f	62
9	1b	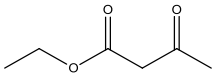	Na/EtOH	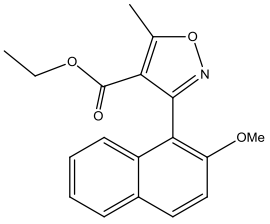 3g	80
10	1b	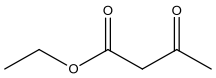	Et_3N	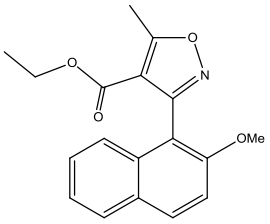 3g	65

11	1b	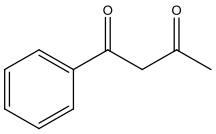	Na/EtOH	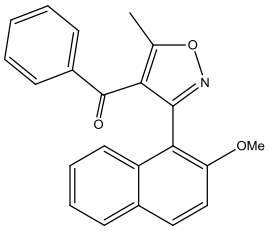 3h	15
12	1b	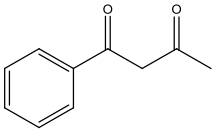	Et_3N	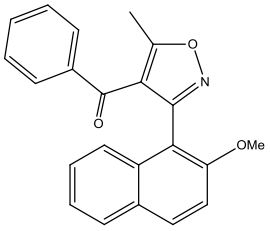 3h	22
13	1b	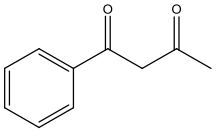	Na/*i*-PrOH	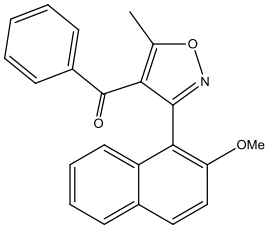 3h	43
14	1b	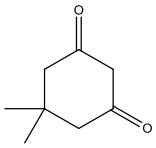	Na/EtOH	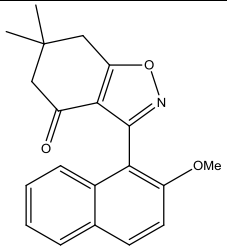 3i	42
15	1b	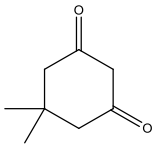	Et_3N	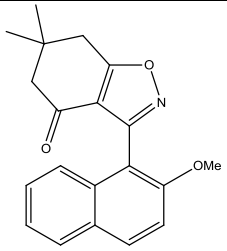 3i	53

16	1b	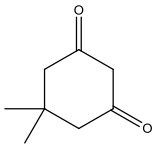	Na/*i*-PrOH	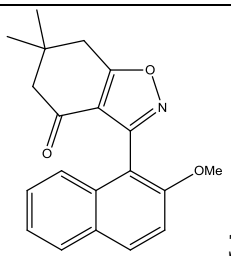 3i	57

The comparison was especially dramatic for the anthryl isoxazole cases, shown in **Table 2**. Excellent yields were obtained for anthryl isoxazoles **3j,** 10-chloro analog **3k**, and 10-bromo analog **3m.** The yields with the enamine procedures were 35-45[16] and 10-20%, for **3j** and **3k**, respectively. **Table 2**, Entry 3 illustrates the direct synthesis of a fused aromatic containing a C-4 tertiary amide, which is an uncommon example of a ketamide used as dipolarophile in the NOC.[22] The ketamide was prepared from diketene and pyrrolidine,[18] and cycloaddition provided the C-4 amide in synthetically reasonable yield. The sluggish reactivity we previously reported for nucleophilic addition to the C-4 ester of the 3-anthryl-isoxazole is exemplified by (1) slow hydrolysis rates (i.e., 60 h using refluxing aqueous LiOH)[9] and (2) the observation that n-BuLi deprotonates the C-5 methyl at -78^{o}C without noticeable addition to the C-4 ester.[19] The C-4 functionalization prior to the NOC stage is a definite advantage for the preparation of AIMs, and will be the subject of further study.

Table 1-2 Nitrile oxide cycloaddition to form hindered 3-anthracenyl-isoxazoles

Entry	Nitrile Oxide	Dipolarophile	Conditions	Product	Yield %
1	1c	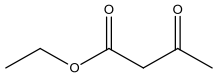	Na/EtOH	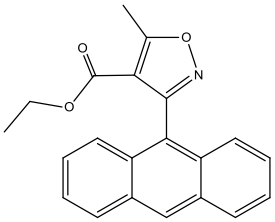 3j	94
2	1d	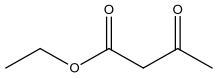	Na/EtOH	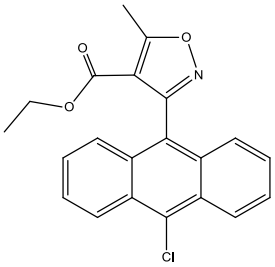 3k	92
3	1c	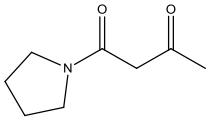	Na/EtOH	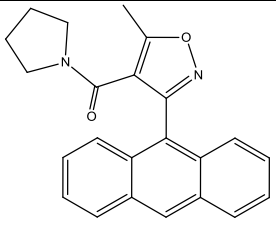 3l	50
4	1e	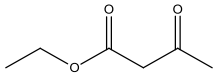	Na/EtOH	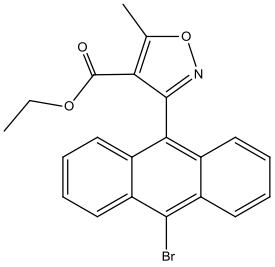 3n	88

5	1e	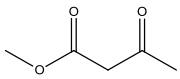	Na/EtOH	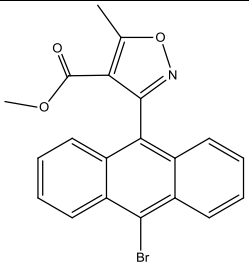 3m	82
6	1e	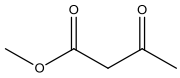	Et_3N	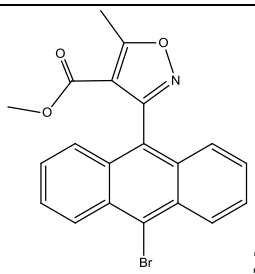 3m	72

In summary, we have found that the *BHMS protocol* produced superior results, especially in sterically encumbered examples containing fused ring aromatic nitrile oxides and that these *conditions represent the methodology of choice* when standard enamine methodology fails. We will report on the chemical and pharmacological application of these novel isoxazoles in due course.

Experimental

General:

All reactions were performed under inert atmosphere. Purification was carried out by column chromatography. Chemicals were purchased from TCI or Aldrich Chemical Company; all commercial reagents are routinely examined for purity by NMR and TLC, and recrystallized or distilled as appropriate. Solvents were reagent grade. Melting points were determined in open capillary tubes on a Melt-Temp apparatus and are uncorrected. NMR spectra were obtained using either a Varian 400 MHz Unity Plus or a Varian NMR systems 500 MHz spectrometer, in deuteriochloroform unless otherwise noted. Infrared

spectra were obtained on a thermo-Nicolet 633 FT-IR spectrometer.

Chemical shifts (δ) are reported using $CHCl_3$ (7.26 ppm for ^1H), $CDCl_3$ (77 ppm for ^{13}C) as references. High resolution mass spectra (HRMS) were obtained using a Micromass electrospray ionization (ESI)/time-of-flight mass spectrometry (LCTOF). Mass spectrometer samples were introduced using a Waters model 2690 separations module HPLC fitted with a C-18 reversed phase column (2.1 mm i.d., 5 cm). Elemental analyses for C, H, and N were performed by Midwest Microlab, Indianapolis, IN. All reactions were monitored by Thin Layer Chromatography (TLC). Purification was performed by flash column chromatography, and analytical samples were prepared by PTLC. Analytical LCMS (UV at 254 nm) and NMR were used to establish the purity of targeted compounds. All compounds that were evaluated in biochemical and biophysical assays had >95% purity as determined by ^1H NMR and LCMS NSC 728558 was prepared from **3k** as previously described.[8,9]

1-(Pyrrolidin-1-yl)butane-1,3-dione.[18] Pyrolidine (0.539 g, 7.5 mmol) is dissolved in 10 mL of anhydrous DCM and diketene (0.925 g, 11.00 mmol) is added. The mixture is stirred at ambient temperature for 2.5 h, followed by removal of the solvent under vacuum to afford (1.163 g, 99%) as red brown liquid. ^1H NMR (500 MHz, $CDCl_3$): δ 3.46 (t, J = 6.62 Hz, 2H), 3.45 (s, 2H), 3.); ^{13}C NMR (125 MHz, $CDCl_3$): δ 202.6, 165.0, 88.8, 51.3, 47.2, 45.9, 30.4, 26.0, 24.4; IR cm^{-1}; mass calculated for $C_8H_{13}NO_2$ 155.0946, found m/z 156.1902 (M +1, 100%).

NOC: sodium enolate method.

(3-(Anthracen-9-yl)-5-methylisoxazol-4-yl)(pyrrolidin-1-yl)methanone, 3l. To a solution of sodium ethoxide, prepared from 0.199 g of Na in 44.2 mL of absolute EtOH,

was added 1-(Pyrrolidin-1-yl)butane-1,3-butane-1,3-dione (1.015 g, 6.54 mmol), and 9-anthrahydroximinoylchloride, (1.06, 4.105 mmol) successively and the resulting red solution was stirred under Ar atmosphere for 4h at ambient temperature. The red-brown solution was extracted with ethyl acetate (4 x 20 mL), washed with DI water (2 x 50 mL) and brine (50 mL), and dried over anhydrous Na_2SO_4. Filtration and concentration afforded the desired product **3l** as red-brown oil (1.40 g, 95%), which was further purified by silica column flash chromatography (Hexanes: EtOAc; 10:1), and PTLC to afford **3l** as off white solid (0.7375 g, 50 %).

NOC: triethyl amine method. **Synthesis of 1-(5-methyl-3-(2-methylnaphthalene-1-yl)isoxazol-4-yl)ethanone, 3a.** To 2,4-pentanedione (0.42 g, 4.11 mmol) in absolute ethanol (21ml) at ambient temperature was added triethylamine (0.47 g, 4.584 mmol) followed by addition of nitrile oxide (0.6 g, 3.28 mmol). The temperature was raised to 53^{o}C and the mixture stirred under Ar atmosphere for 72 h. The pale yellow solution was extracted with chloroform (4 x 20 mL), washed with DI water (2 x 50 mL) and brine (50 mL), dried over anhydrous Na_2SO_4. Filtration, concentration and silica column flash chromatography (Hexanes: EtOAc: DCM; 5:1:1) afforded the desired product **3a** (0.289 g, 40 %):

Analytical data for 3-fused aryl isoxazole products.

1-(5-Methyl-3-(2-methylnaphthalene-1-yl)isoxazol-4-yl)ethanone, 3a. Oil, TLC SiO_2 hexane-DCM-EtOAc 4:1:1 R_f 0.77. ^{1}H NMR (500 MHz, $CDCl_3$) δ 7.80-7.75 (m, 2H), 7.38-7.32 (m, 4H), 2.76 (s, 3H), 2.26 (s, 3H), 1.56 (s, 3H); ^{13}C NMR (125 MHz, $CDCl_3$) δ 192.3, 175.7, 159.6, 135.3, 132.3, 131.4, 129.5, 127.8, 126.8, 125.2, 124.0, 117.5, 28.6, 19.8, 13.6; HRMS Calc'd for $C_{17}H_{16}NO_2$ 266.1181; Found: 266.1193.

Ethyl 3-(2-methylnaphthalen-1-yl)-5-methylisoxazole-4-carboxylate, 3b. Oil, TLC SiO_2 hexane-DCM-EtOAc 4:1:1 R_f 0.6. ^{1}H-NMR ($CDCl_3$) d 7.826 (d, 2H); 7.25-7.398(m, 4H); 3.87 (q, 2H); 2.841 (s, 3H); 2.303 (s, 3H); 0.651 (t, 3H). ^{13}C NMR (125 MHz, $CDCl_3$) δ 175.7, 161.4, 160.7, 135.0, 132.5, 131.4, 128.9, 127.9, 127.7, 126.2, 124.8, 124.6, 124.5, 110.1, 59.9, 20.1, 13.2, 13.0. HRMS calc'd for $C_{18}H_{18}NO_3$: 296.1287; Found: 296.1297.

Phenyl (5-methyl-3-(2-methylnaphthalen-1-yl)isoxazol-4-yl)methanone, 3c. Oil, TLC SiO_2 hexane-DCM-EtOAc 4:1:1 R_f 0.79 ^{1}H NMR (500 MHz, $CDCl_3$): δ 7.65 (d, J = 7.90, 1H), 7.60 (d, J = 8.50 Hz, 1H), 7.55 (d, J = 8.00 Hz, 1H), 7.37 (t, J = 6.60 Hz, 1H), 7.33 (m, 3H), 7.16 (m, 2H), 6.94 (t, J = 8.00 Hz, 2H), 3.38 (s, 3H), 2.64 (s, 3H); ^{13}C NMR (125 MHz, $CDCl_3$): δ 189.8, 173.7, 171.0, 160.3, 137.1, 135.5, 132.4, 132.3, 131.4, 129.3, 129.2, 128.1, 128.0, 127.9, 127.8, 127.5, 125.0, 124.5, 124.4, 123.6, 117.8, 20.4, 14.0; HRMS Calc'd for $C_{22}H_{18}NO_2$: 328.1338; Found: 328.1370.

6,6-Dimethyl-3-(2-methylnaphthalen-1-yl)-6,7-dihydrobenzo[*d*]isoxazol-4(5*H*)-one 3d. Oil, TLC SiO_2 hexane-DCM-EtOAc 4:1:1 R_f 0.71. ^{1}H NMR (500 MHz, $CDCl_3$) δ 7.87 (d, J = 8.3, 1H), 7.84 (d, J = 8.3, 1H), 7.36-7.43 (m, 4H), 3.01 (s, 2H), 2.40 (d, J = 8.3, 2H), 2.31 (s, 3H), 1.22 (s, 3H), 1.19 (s, 3H); ^{13}C NMR (125 MHz, $CDCl_3$) δ 190.8, 180.9, 171.1, 157.9, 135.6, 132.3, 131.7, 129.7, 129.6, 128.4, 128.2, 128.1, 128.0, 125.2, 125.0, 124.5, 124.3, 122.9, 52.4, 37.0, 35.5, 28.6, 28.5, 28.1, 28.0, 21.0, 14.2. HRMS Calc'd for $C_{20}H_{20}NO_2$: 306.1494; Found: 306.1516.

1-(3-(2-methoxynaphthalene-1-yl)-5-methylisoxazol-4-yl)ethanone, 3e. Oil, TLC SiO_2 hexane-DCM-EtOAc 4:1:1 R_f 0.53. ^{1}H NMR (500 MHz, $CDCl_3$) δ 8.01 (d, J = 9.30 Hz, 1H), 7.84 (d, J = 7.80 Hz, 1H), 7.48 (d, J = 8.30 Hz, 1H), 7.44 (t, J = 8.30 Hz, 1H), 7.39

(d, *J* = 7.90 Hz, 1H), 7.36 (d, *J* = 8.80 Hz, 1H), 3.90 (s, 3H), 2.81 (s, 3H), 1.76 (s, 3H); ^{13}C NMR (125 MHz, $CDCl_3$) δ 193.2, 175.4, 157.7, 155.3, 133.3, 132.1, 128.7, 128.1, 127.8, 124.2, 123.9, 118.3, 112.6, 111.4, 56.4, 28.8, 14.0. HRMS Calc'd for M+H, $C_{17}H_{16}NO_3$ 282.1130; Found: 282.1150 (M +1, 100%). Anal Calc'd for $C_{17}H_{15}NO_3$: C, 72.58; H, 5.37; N, 4.98. Found: C, 71.81; H, 5.52; N, 4.56.

Methyl 3-(2-methoxynaphthalene-1-yl)-5-methylisoxazole-4-carboxylate, 3f. Oil, TLC SiO_2 hexane-DCM-EtOAc 4:1:1 R_f 0.56. ^{1}H NMR (500 MHz, $CDCl_3$): δ 7.96 (d, *J* = 9.05 Hz, 1H), 7.82 (d, *J* = 9.99 Hz, 1H), 7.55 (d, *J* = 9.99 Hz, 1H), 7.40 (t, *J* = 9.99 Hz, 1H), 7.35 (t, *J* = 9.99 Hz, 2H), 3.86 (s, 3H), 3.54 (s, 3H), 2.81 (s, 3H); ^{13}C NMR (500 MHz, $CDCl_3$): δ 175.1, 162.1, 158.5, 155.3, 133.0, 131.3, 128.6, 127.9, 127.0, 124.0, 123.6, 112.6, 111.4, 110.4, 56.4, 51.3, 13.3; IR cm^{-1}; HRMS Calc'd for $C_{17}H_{16}NO_4$: 298.1079; Found 298.1111. Anal. Calc'd for $C_{17}H_{15}NO_4$: C, 68.68; H, 5.09; N, 4.71. Found: C, 66.81; H, 5.00; N, 4.53.

Ethyl 3-(2-methoxynaphthalen-1-yl)-5-methylisoxazole-4-carboxylate, 3g, as yellow solid (1.8 g, 60 %): mp 103-104^{o}C; ^{1}H NMR (500 MHz, $CDCl_3$): δ 7.96 (d, *J* = 8.99 Hz, 1H), 7.81 (d, *J* = 8.07 Hz, 1H), 7.50 (d, *J* = 8.55 Hz, 1H), 7.39 (dd, *J* = 11.00, 6.84 Hz 1H), 7.34 (d, *J* = 9.05 Hz, 2H), 3.96 (q, *J* = 7.06 Hz, 2H), 3.88 (s, 3H), 2.82 (s, 3H), 0.79 (t, *J* = 7.06 Hz, 3H); ^{13}C NMR (125 MHz, $CDCl_3$): δ 175.3, 161.9, 158.6, 155.3, 133.3, 131.3, 128.6, 127.9, 127.1, 124.1, 123.7, 112.7, 111.8, 110.6, 60.1, 56.5, 13.5, 13.3; ESI-MS Calculated for $C_{18}H_{17}NO_4$+H m/z 312.1428 (M +1, 100 %). Anal Calc'd for $C_{18}H_{17}NO_4$: C, 69.44; H, 5.50; N, 4.50. Found: C, 69.58; H, 5.47; N, 4.54.

Phenyl (3-(2-methoxynaphthalen-1-yl)-5-methylisoxazol-4-yl) methanone, 3h. mp 141-142 ^{o}C; ^{1}H NMR (500 MHz, $CDCl_3$): δ 8.06 (d, *J* = 8.50, 1H), 7.73 (d, *J* = 8.80 Hz,

2H), 7.51 (t, *J* = 8.40 Hz, 1H), 7.44 (d, *J* = 8.30 Hz, 2H), 7.36 (t, *J* = 7.55 Hz, 1H), 6.96 (t, *J* = 7.80 Hz, 2H), 6.90 (d, *J* = 9.30 Hz, 1H), 3.61 (s, 3H), 2.69 (s, 3H); ^{13}C NMR (125 MHz, $CDCl_3$): δ 189.8, 173.2, 157.8, 154.5, 137.1, 132.7, 132.4, 131.7, 128.7, 128.5, 128.0, 127.7, 127.5, 124.2, 117.6, 111.6, 78.1 55.5, 29.7; ESI-MS for $C_{22}H_{17}NO_3$+Hm/z 344.1008 (M +1, 100%).

6,6-dimethyl-3-(2-methoxynaphthalen-1-yl)--6,7-dihydrobenzo[*d*]isoxazol-4(5H)-one, 3i. Oil, TLC SiO_2 hexane-DCM-EtOAc 4:1:1 R_f 0.46. ^{1}H NMR (500 MHz, $CDCl_3$) δ 7.96 (d, *J* = 9.1, 1H), δ 7.81 (d, *J* = 7.8 Hz, 1H), 7.69 (d, *J* = 8.6 Hz, 1H), 7.43 (dt, *J* = 9.8 Hz, 1.5 Hz, 1H), 7.36 (dd, *J* = 6.8 Hz, 1.3 Hz, 1H), 7.34 (d, *J* = 9.3 Hz, 2H), 3.85 (s, 3H), 2.90 (s, 2H), 2.36 (q, *J* = 14.7 Hz, 2H), 1.17 (s, 3H), 1.14 (s, 3H); ^{13}C NMR (125 MHz, $CDCl_3$) δ 190.7, 180.2, 155.7, 155.4, 132.6, 131.7, 131.6, 128.6, 128.1, 128.0, 127.9, 127.8, 127.6, 127.2, 126.9, 123.9, 123.7, 123.4, 115.2, 112.9, 112.8, 112.6, 109.9, 56.4, 56.2, 52.3, 36.7, 35.1, 28.3, 28.0. HRMS Calculated for $C_{20}H_{20}NO_3$ 322.1443; Found: 322.1458.

Ethyl 3-(anthracen-9-yl)-5-methylisoxazole-4-carboxylate, 3j. mp 121-122^{o}C; TLC SiO_2 hexane-EtOAc 10:1, R_f 0.30. ^{1}H NMR (500 MHz, $CDCl_3$): δ 8.58 (s, 1H), 8.05 (d, *J* = 8.31 Hz, 2H), 7.65 (d, *J* = 8.55 Hz, 2H), 7.40-7.49 (m, 4H), 3.71 (q, *J* = 7.21 Hz, 2H), 2.93 (s, 3H), 0.32 (t, *J* = 7.10 Hz, 3H); ^{13}C NMR (500 MHz, $CDCl_3$): 176.2, 161.5, 160.5, 131.0, 130.8, 128.7, 128.5, 126.3, 125.4, 125.2, 122.7, 111.4, 60.1, 13.5, 12.8, spectral data are in accord with those reported previously.[16a] ESI-MS for $C_{21}H_{17}NO_3$+H m/z 332.1441 (M +1, 100%).

Ethyl 3-(10-chloroanthracen-9-yl)-5-methylisoxazole-4-carboxylate, 3k. mp 123-124^{o}C, lit. mp 119-120.[16b] TLC SiO_2 hexane-EtOAc 10:1, R_f 0.28. ^{1}H NMR (500 MHz,

$CDCl_3$): δ 8.59 (d, J = 8.80 Hz, 2H), 7.53 - 7.60 (m, 4H), 7.43 (d, J = 8.80 Hz, 2H), 3.72 (q, J = 7.1 Hz, 2H), 2.93 (s, 3H), 0.39 (t, J = 7.1 Hz, 3H); ^{13}C NMR (500 MHz, $CDCl_3$): 177.3, 161.3, 161.2, 134.1, 131.1, 128.3, 126.7, 125.9, 125.1, 122.6, 111.5, 60.2, 13.2; ESI-MS for $C_{21}H_{16}ClNO_3$+H m/Z 366.0886 (M +1, 95%).

[3-(Anthracen-9-yl)-5-methylisoxazol-4-yl](pyrrolidin-1-yl)methanone, 3l. mp 194-5^{o}C. ^{1}H NMR (500 MHz, $CDCl_3$): δ 8.54 (s, 1H), 7.99 (d, J = 9.29 Hz, 2H), 7.95 (d, J = 10.0 Hz, 2H), 7.48-7.45 (m, 4H), 3.10 (t, J = 6.87 Hz, 2H), 2.73 (s, 3H), 2.60 (t, J = 6.61 Hz, 2H), 1.42 (pentet, J = 6.85 Hz, 2H), 1.29 (pentet, J = 6.60 Hz, 2H); ^{13}C NMR (125 MHz, $CDCl_3$): δ 170.1, 161.3, 158.3, 131.0, 130.5, 129.4, 128.5, 126.9, 126.7, 125.8, 125.3, 125.0, 121.9, 116.5, 47.7, 45.3, 25.6, 23.7, 12.4; ESI-MS for $C_{23}H_{20}N_2O_2$+H, m/z 357.0757 [M +1, (100)]. Anal Calc'd for $C_{23}H_{20}N_2O_2$: C, 77.51; H, 5.66; N, 7.86. Found: C, 77.37; H, 5.45; N, 7.99.

Methyl 3-(10-bromoanthracen-9-yl)-5-methylisoxazole-4-carboxylate, 3m. Rf=0.45 Hex:EtOAc:DCM 4:1:1^{1}H NMR (500 MHz, $CDCl_3$): 8.63-8.60 (d,2H), 7.62-7.59 (m,4H), 7.47-7.43 (m,2H), 3.32 (s,3H), 2.93 (s,3H). ^{13}C NMR (125 MHz, $CDCl_3$): 176.08, 163.32, 161.53, 131.12, 129.90, 127.96, 126.88, 126.39, 125.60, 123.12, 51.35, 13.42. HRMS Calc'd for M+H $C_{20}H_{14}NO_3{}^{79}Br$+H, m/z 396.0227; Found: 396.0235.

Laser Scanning Cytometry Methods: SNB-19 human glioblastoma cells (American Type Cell Culture Cat No. CRL-2266) were plated at a density of 2000 cells/mL on cover slips in RPMI medium (with L-glutamine and penicillin/streptomycin and supplemented with 10% fetal bovine serum). Cell culture medium and supplements were obtained from VWR (West Chester, PA). The cells were incubated at 37 °C under a humidified atmosphere containing 5% CO_2 and allowed to adhere. Medium was aspirated and

replaced with 1 μM NSC 728558 for 24-h exposure. Drug was removed and cells were washed twice with phosphate buffered saline (PBS). Cells were fixed in 4% paraformaldehye (15 min, 21 °C) and washed once with PBS. Following two additional washes, slides were inverted to microscope slides and sealed using FluorSave Reagent (Calbiochem). Images were generated from scans from a CompuCyte iCys Laser Scanning Cytometer. (CompuCyte, Westwood, MA). Cells were scanned with a 405 nm 30 mW Diode laser. Fluorescent signals were measured in photo-multiplier detectors following a 440/30 Band-pass (BP) filter to detect NSC 728558 presence. Light absorption was also measured to produce a differential interference contrast (DIC)-like image for cell morphology. Each signal was given a pseudo-color and overlaid to produce images.

Acknowledgement

The authors thank the NIH for grants R21NS067466, P20RR017670 and P30NS055022 for financial support of this work.

References and notes

1. (a) Zhu, S.; Shi, S.; Gerritz, S.W. *Tetrahedron Lett*. **2011**, *52,* 4001-4004. References 1-4 of this paper reviews recent bioactive isoxazoles in the patent literature. (b) Nakamura, M.; Kurihara, H.; Suzuki, G.; Mitsuya, M.; Ohkubo, M.; Ohta, H. *Bioorg. Med. Chem. Lett.*, **2010**, *20*, 726-729.

2. The Kurth group has provided a useful catalog of the bioactive isoxazole literature in their NOC synthesis papers over the years, the following are illustrative examples: (a) Yu, G.J.; Yang, B.; Verkman, A. S.; Kurth, M. J**.** *Synlett* **2010**, *7*, 1063-1066. (b) Meng, L.; Lorsbach, B.A.; Sparks, T.C.; Fettinger, J.C.; Kurth, M.J. *J. Comb. Chem.*

2010, *12*, 129-136. (c) Butler, J.D.; Donald, M.B.; Ding, Z.; Fettinger, J.C.; Kurth, M.J. *Tetrahedron Lett.* **2009**, *50*, 5110-5112. (d) Choung, W.; Lorsbach, B.A.; Sparks, T.C.; Ruiz, J. M.; Kurth, M.J. *Synlett* **2008**, *19*, 3036-3040. (e) Quan, C.; Kurth, M. *J. Org. Chem*. **2004**, *69*, 1470-1474 (f) Hwang, S.H.; Kurth, M.J. *J. Org. Chem*. **2002**, *67*, 6564-6567.

3. In the course of their studies on glutamate receptor and transporter ligand pharmacology, the Krogsgaard-Larsen group has greatly expanded the tool box for isoxazole synthesis: Egebjerg, J.; Schousboe, A.; Krogsgaard-Larsen, P., Eds. *Glutamate and GABA Receptors and Transporters, Structure Function and Pharmacology.* Taylor and Francis: NY, NY, **2002**.

4. Pinho e Melo, T. M.V.D. *Current Org. Chem.*, **2005**, *9*, 925-958.

5. Trogu, E.; Cecchi, L.; De Sarlo, F.; Guideri, L.; Ponticelli, F.; Machetti, F. *Eur. J. Org. Chem.* **2009**, 5971–5978, and cited references.

6. Bode, J. W.; Hachisu, Y.; Matsuura, T.; Suzuki, K. *Org. Lett*., **2003**, 5, 391-394.

7. Bode, J.W.; Hachisu, Y.; Matsuura, T.; Suzuki, K. *Tetrahedron Lett.* **2003**, *44*, 3555–3558.

8. Han, X.; Li, C.; Mosher, M.D.; Rider, K.C.; Zhou, P.; Crawford, R.L.; Fusco, W.; Paszczynski, A.; Natale, N. R. *Bioorg. Med. Chem*. **2009**, *17*, 1671-1680.

9. Gajewski, M.P.; Beall, H.; Schnieder, M.; Stranahan, S. M.; Mosher, M. D.; Rider, K. C.; Natale, N. R. *Bioorg. Med. Chem*. *Lett.* **2009**, *19*, 4067-4069.

10. (a) Veiseh, M.; Gabikian, P.; Bahrami, S.-B.; Veiseh, O.; Zhang, M.; Hackman, R. C.; Ravanpay, A.C.; Stroud, M. R.; Kusuma, Y.; Hansen, S.J.; Kwok, D.; Munoz, N. M.; Sze, R.W.; Grady, W.M.; Greenberg, N. M.; Ellenbogen, R. G.; Olson, J. M.

Cancer Res. **2007**; *67*: 6882-6888. (b) Smeltzer, C.; Cannon, M.J.; Pinson, P.; Munger, J.S.; West, F.G.; Grissom, C.B. *Org. Lett*. **2001,** *3,* 799-801. (c) McGreevy, J. M.; Cannon, M.; Grissom, C. B. *J. Surg. Res.* **2003,** *111,* 38-44.

11. Feuer, H., Ed, *Nitrile Oxides, Nitrones and Nitronates in Organic Synthesis*, John Wiley & Sons, Inc., Hoboken, New Jersey, 2008.
12. (a) Stork, G.; McMurry, J.E. *J. Am. Chem. Soc.* **1967**, *89,* 5461- 5462. (b) McMurry, J.E. *Org. Synth.* **1988**, *Coll. Vol. VI,* 582-594.
13. Natale, N.R.; McKenna, J.I.; Niou, C.-S.; Borth, M.; Hope, H. *J. Org. Chem.*, **1985**, *50,* 5660-6.
14. Zamponi, G.; Stephanie C. Stotz, Richard J. Staples, Rogers, T.A.; Nelson, J.K.; Hulubei, V.; Blumenfeld, A.; Natale, N.R. *J. Med. Chem.,* **2003**, *46,* 87-96, and cited references.
15. Bowles, K.D.; D.A. Quincy, D.A; Mallet, B.; McKenna, J.I.; Natale, N.R. *J. Chem. Ed.*, **1985**, *62,* 1118-20.
16. (a) Mosher, M.D.; Natale, N.R. *J. Hetereocycl. Chem.*, **1995**, *32*, 779-781. (b) Han, X.; Twamley, B.; Natale, N.R. *J. Heterocycl. Chem.*, **2003**, *40,* 539-545.
17. Grundmann, C.; Dean, J.M. *J. Org. Chem*., **1965**, *30*, 2809-2812.
18. (a) Beger, J.; Thielemann, C. *J. Praktische Chem*., **1981**, *323,* 337-344. (b) Fujisawa, T.; Sato, T.; Takeuchi, M. *Chem. Lett*., **1982**, *1*, 71-74.
19. Han, X.; Li, C.; Rider, K.C.; Blumenfeld, A.; Twamley, B.; Natale, N.R. *Tetrahedron Lett.*, **2002**, *43*, 7673-7677.
20. (a) Renzi, G.; Dal Piaz, V. *Gazz. Chim. It.,* **1965**, *95,* 1478-1491. (b) Renzi, G.; Pinzauti, S. *Il Farmaco Ed. Sci.*, **1969**, *24*, 885-892.

21. (a) Liu, B.; Liu, G.; Xin, Z.; Serby, M.D.; Zhao, H.; Schaefer, V.G.; Falls, D.; Kaszubska,_ W.; Collins, C.A.; Sham, H. L. *Bioorg. Med. Chem. Lett*. **2004**, *14*, 5223–5226 (b) Xin, Z.; Zhao, H.; Serby, M.D.; Liu, B.; Schaefer, V.G.; Falls, D.H.; Kaszubska, W.; Colins, C.A.; Sham, H.L.; Liu, G. *Bioorg. Med. Chem. Lett*. **2005**, *15*, 1201–1204.

22. Butler, J.D.; Coffman, K.C.; Ziebart, K.T.; Toney, M.D.; Kurth, M.J. *Chem. Eur J*., **2010**, *16*, 9002-9005

Supplementary Material

Representative HPLC trace for **3m**. Characterization data for by-products **7** and **8**, representative spectra for products **3**.

7b. R_f 0.11. ESI- MS Calculated for $C_{16}H_{18}N_2O_2$ FW 270, observed m/z 271 [M $+1^+$100% Rel. I.].

8b. R_f 0.05. ESI- MS Calculated for $C_{24}H_{18}N_2O_2$ FW 366, observed m/z 367 [M $+1^+$ 80% Rel. I.]; 733 (100).

8g. mp 177-178 ^oC; ^1H NMR (500 MHz, $CDCl_3$): δ 8.09 (t, J = 8.68 Hz, 1H), 8.03 (d, J = 9.05 Hz, 2H), 7.87 (t, J = 8.32 Hz, 3H), 7.56-7.49 (m, 2H), 7.44-7.39 (m, 4H), 4.06 (s, 3H), 4.02 (s, 3H); ^{13}C NMR (125 MHz, $CDCl_3$): δ 174.0, 165.7, 157.5, 156.5, 134.0, 133.3, 132.7, 132.4, 128.7, 128.6, 128.3, 128.2, 128.1, 127.6, 124.4, 124.3, 124.2, 124.0, 113.2, 112.9, 110.3, 107.7, 57.0, 56.8.

7k. ESI- MS Calculated for $C_{19}H_{17}{}^{35}ClN_2O_2$ FW 340.10, observed m/z 341.6145 [$C_{19}H_{17}{}^{35}ClN_2O_2$, M $+1^+$ 100% Rel. I.], 343.6289 [$C_{19}H_{17}{}^{37}ClN_2O_2$, 37].

Fig. 1-2. HPLC trace for **3m**

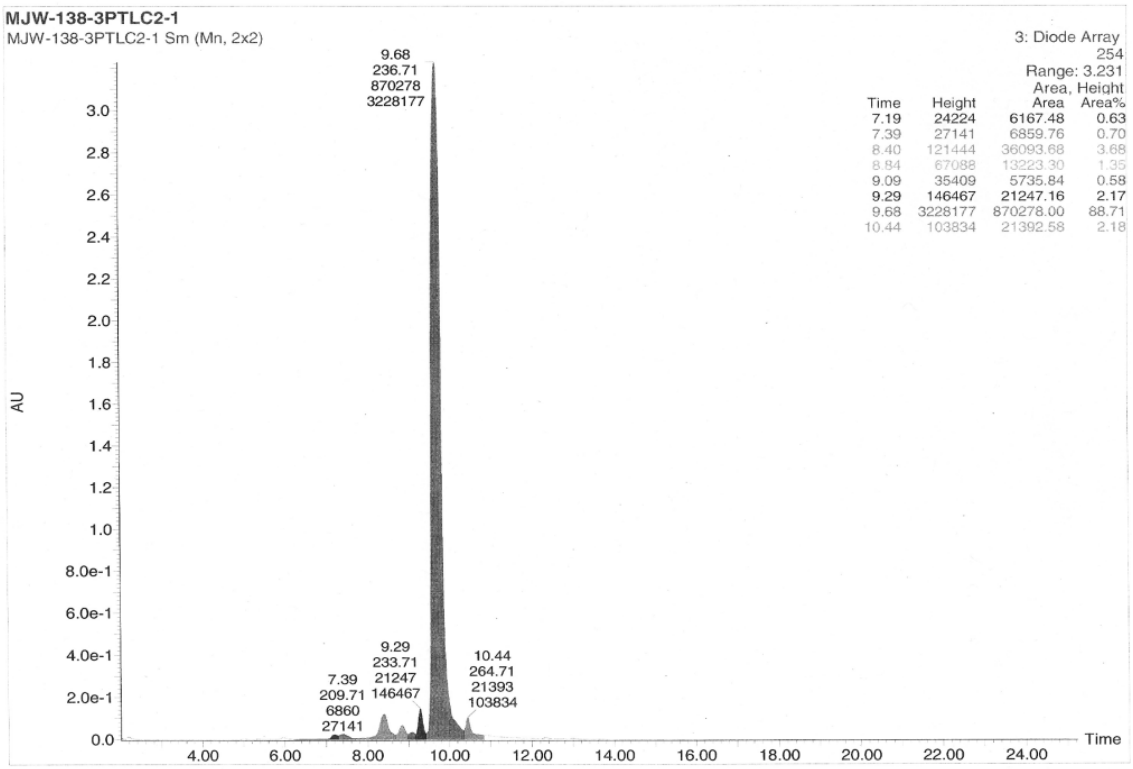

Fig. 1-3. Proton spectrum for **3m**

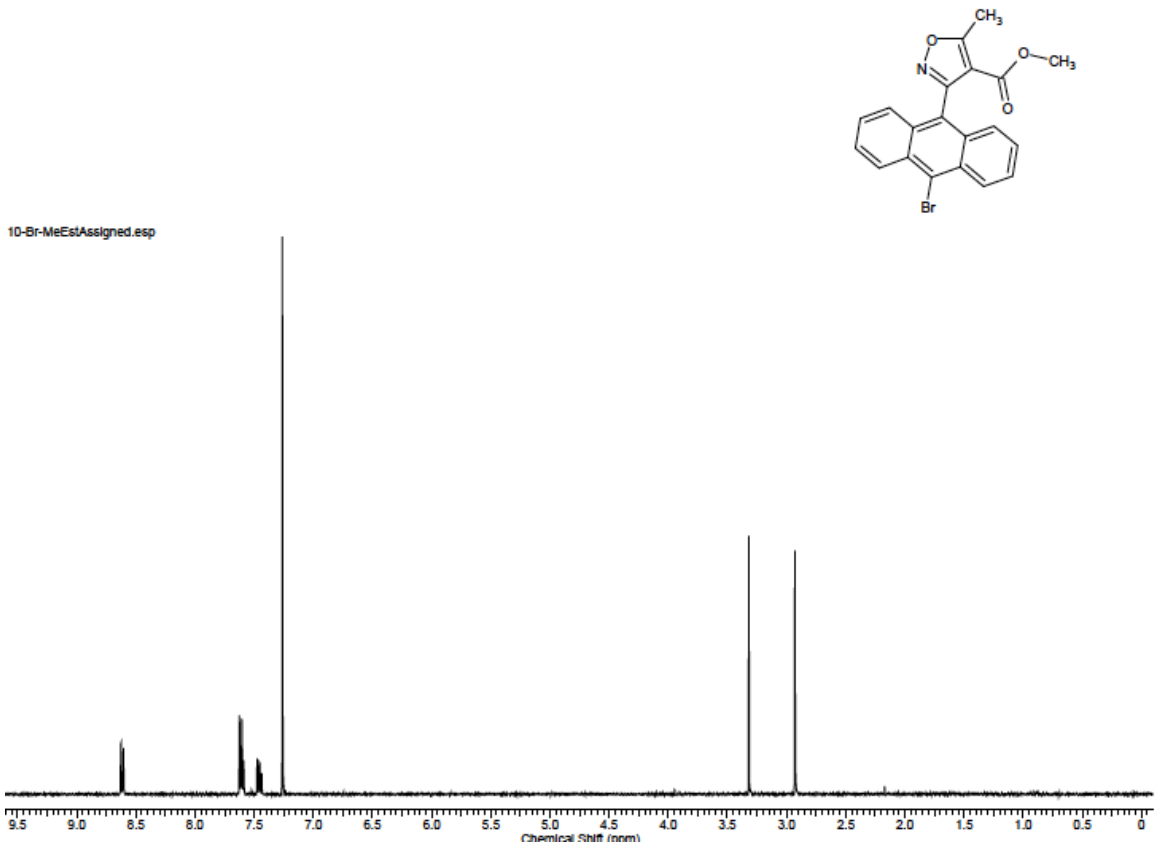

Fig. 1-4. Carbon spectrum for **3m**

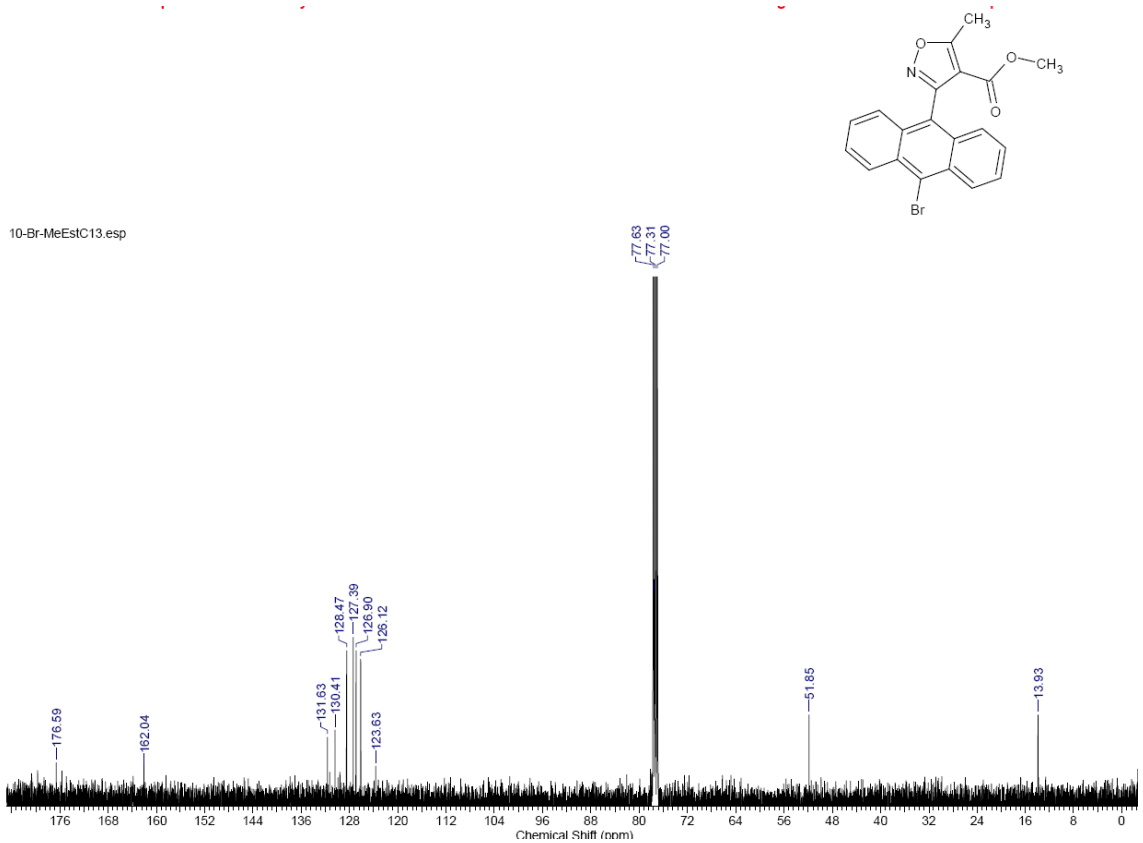

Fig. 1-5. Proton spectrum for **7k**

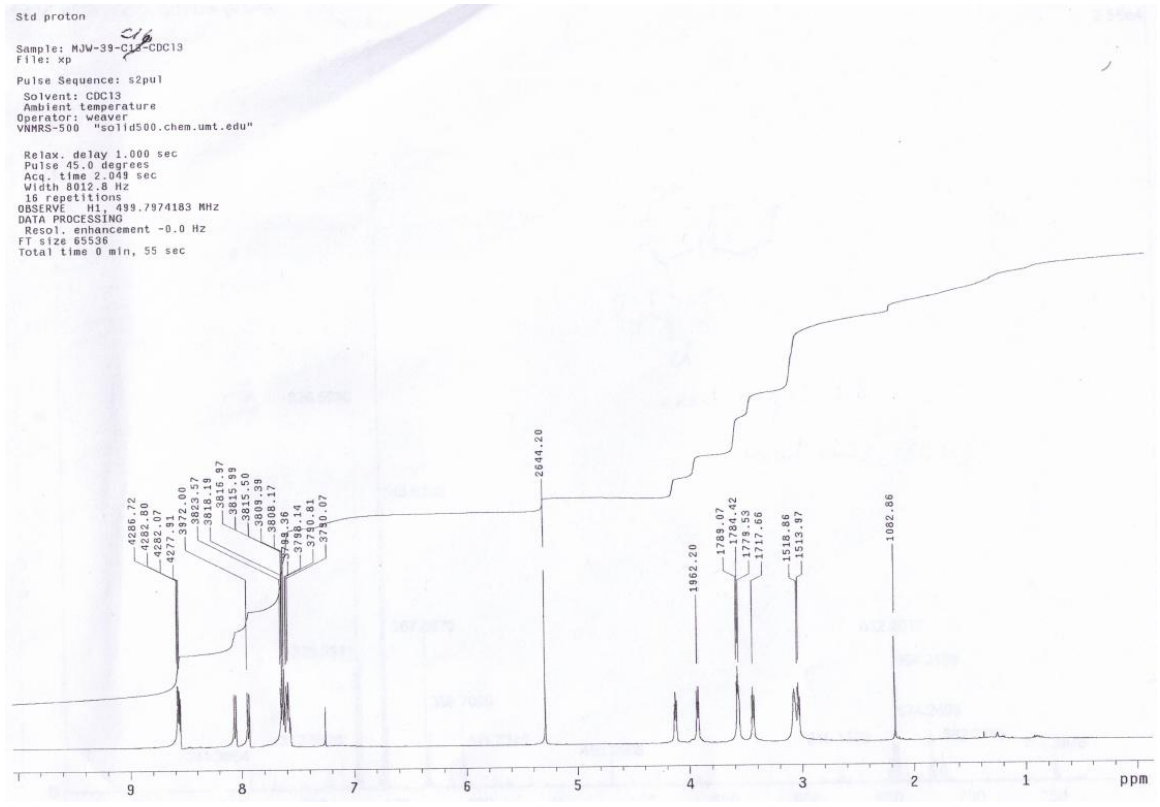

Chapter 2: Crystal Structure of Ethyl 3-(10'-bromo-9'-anthracenyl)-5-methyl-4-isoxazolcarboxylate

This manuscript will be submitted for publication to Acta Crystrallographica

The title compound adopts a conformation in which the isoxazole and anthryl mean planes are slightly deviated from the orthogonal. The aromatic anthracene ring is fairly planar, and the isoxazole is almost completely planar. The dihedral angle between the carbonyl and isoxazole of is indicative of resonance, also reflected in the bond-length. The isoxazole ethyl ester resides over the shielding cone of the anthryl, which is maintained in solution as evidenced by magnetic anisotropy of the average conformation at room temperature.

Fig. 2-1. Crystal structure of title compound

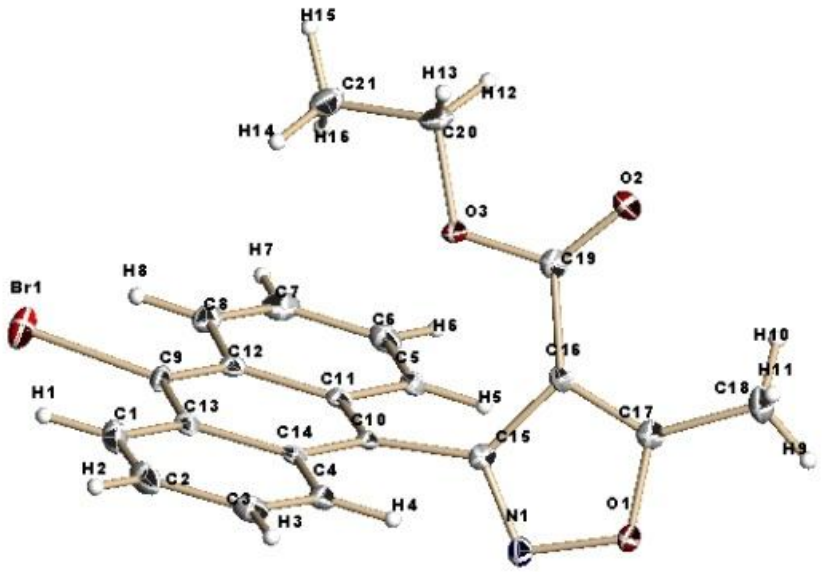

Related literature

For the synthesis of anthryl isoxazoles, see: Mosher and Natale (1995); Zhou, *et al.* (1997); Han and Natale, (2001); Rider, *et al.* (2010); Mirzaei, *et al.* (2012). For previous studies on anthryl isoxazole crystallography, see: Mosher (1996); Han, (2002); Han, (2003); Li, (2006); Li (2008). For the antitumor activity of aryl isoxazole amides (AIMs), see: Han, *et al.* (2009); Gajewski, *et al* (2009).

Acknowledgment

The Bruker single crystal x-ray diffractometry facility at Ithaca College was established with support of the Department of Chemistry. NRN, MJC, MJW and ND thank the National Institutes of Health for grants NINDS P20RR015583 Center for Structural and Functional Neuroscience (CSFN) and P20 RR017670 Center for Environmental Health Sciences (CEHS), and the University of Montana Grant Program.

References

Bruker (2008). APEX2, SAINT and SADABS. Bruker AXS Ins., Madison, Wisconsin, USA.

1. Han, X.; Li ,C.; Mosher, M.D.; Rider, K.C.; Zhou, P.; Crawford R.L.; Fusco, W.; Paszczynski, A.; Natale, N.R. *Bioorg. Med. Chem.* **2009**, *17*, 1671-1680.
2. Gajewski, M.P.; Beall H, Schnieder M., Stranahan S.M.; Mosher, M.D., Rider K.C., Natale, N.R. *Bioorg. Med Chem. Lett.* **2009**; *19*, 4067-4069.
3. Kohn, K.W.; Zeeberg, B.R.; Reinhold, W.C.; Sunshine, M.; Luna, A.; Pommier, Y. Gene Expression Profiles of the NCI-60 Human Tumor Cell Lines Define Molecular Interaction Networks Governing Cell Migration Processes. *PLoS ONE*, **2012**, *7*: e35716. doi:10.1371/journal.pone.0035716

4. Shoemaker, R.H. The NCI60 human tumour cell line anticancer drug screen. *Nature Reviews Cancer,* **2006,** *6,* 816-823.

5. Boyd, M. R. Status of the NCI Preclinical Antitumor Drug Discovery Screen. *Principles Pract. Oncol*. **1989**, 3, 1.

6. Balasubramanian, S.; Hurley, L.H.; Neidle, S. Targeting G-quadruplexes in gene promoters: a novel anticancer strategy? *Nature Reviews*, **2011**, *10*, 261-275.

7. *Therapeutic Applications of Quadruplex Nucleic Acids*, Stephen Neidle, (Elsevier/Academic Press, Amsterdam, 2012).

8. Li, C.; Twamley, B.; Natale, N.R. Preparation and Crystal Structures of Two 3-Anthracenyl Isoxazolyl Sulfonamides. *J. Heterocycl. Chem*., **2008**, *45*, 259-264.

9. Li, C.; Twamley, B.; Natale, N.R. Ethyl 3-(10-chloroanthracenyl)-5-(1-phenyl-2-hydroxyethenyl)isoxazole-4-carboxylate: an enol produced by Dess–Martin oxidation Acta Cryst. **2006.** ***E****62***,** o854–o856.

10. Han, X., Twamley, B., Natale, N. R. Preparation of 3-(10'-Halo-9'-anthracenyl)-5-methyl isoxazolecarboxylic Esters *J. Heterocycl. Chem.,* **2003**, *40,* 539-545.

11. Han, X., Li, C., Rider, K. C., Blumenfeld, A., Twamley, B., Natale, N. R. The Isoxazole as a linchpin for molecules which target folded DNA conformations: Selective Lateral Lithiation and Palladation. *Tetrahedron Lett.*, **2002**, *43*, 7673-7677.

12. Mosher, M. D., Natale, N. R., Vij, A. Intercalating Isoxazoles. *Acta Cryst.*, **1996**, *C52*, 2513-2515.

13. Mirzaei, Y.R., Weaver, M.W., Steiger, S.A., Kearns, A.K., Gajewski, M.P., Rider, K.C., Beall, H.D., Natale, N.R., Improved synthesis of 3-aryl isoxazoles containing fused aromatic rings. *Tetrahedron*. **2012,** 68, 10360-10364.

Supplementary Materials

Comment

The aryl isoxazole amides (AIMs)[1,2] have significant activity in the National Cancer Institute's 60 cell line screen, [3,4] comparable to several agents in general medical practice, such as fluorouridine and bleomycin.[5] Our working hypothesis for developing the structure activity relationship (SAR) of AIMs to improve their anti-tumor efficacy is focused on the quadruplex DNA conformations.[6,7] To more accurately inform our G-4 - small molecule docking studies, we rely on crystallographic determinations of AIMs. In previous studies we have determined that the dihedral angle between the isoxazole and the C-3 aryl is approximately orthogonal, and we have postulated that this is a critical feature in the biological activity of the AIMs. For example, the anthracenyl group is almost perpendicular to the isoxazole plane, in Ethyl 3-(10-chloroanthracenyl)-5-(1-phenyl-2-hydroxylethylenyl)isoxazole-4-carboxylate 85.51(4),[8] which is similar to analogous anthracenyl isoxazole structures in the Cambridge Structural Database, i.e. ethyl 3-(10'-chloro-9'-anthracenyl)-5-methyl-4-isoxazolcarboxylate, 74.3 (Han et al., 2003; CSD refcode EZENEC),[10] ethyl 3-(10'-chloro-9'-anthracenyl)-5-(2-phenylethyl)-4-isoxazolecarboxylate, 78.5 (Han et al., 2002; CSD refcode MUQMOA),[11] This AIM analog represents a key intermediate in future synthesis and SAR studies, and our progress will be reported in due course.

Experimental Section

To a suspension of anthracene-9-carbaldehyde (2.0 g, 9.7 mmol) in dichloromethane (70 mL) was added a solution of bromine (1.86 g, 11.64 mmol) in dichloromethane (6 mL) at room temperature. The solution was then brought to reflux and allowed to stir for 4

hours. The temperature was decreased to -5 °C and stirring continued for another 30 minutes. The precipitate was filtered and washed with cold hexanes to afford 2.2 g (80 %) of a brown solid. The precipitate was purified via crystallization from $CHCl_3$ to yield 1.9 g (70%) pure 10-bromoanthracene-9-carbaldehyde. ^{1}H NMR ($CDCl_3$) δ 11.51 (s, 1H), 8.90 (m, 2H), 8.68 (m, 2H), 7.69 (m, 4H).

To a solution of 10-bromoanthracene-9-carbaldehyde in THF: EtOH: H2O (12 mL: 6 mL: 6 mL) was dissolved sodium acetate (1.9 g, 15.78 mmol) and hydroxylamine hydrochloride (0.8 g, 10.53 mmol). The reaction was allowed to stir at room temperature for 4 days. After 24 hours a large amount of bright yellow precipitate had formed. The mixture was placed under reduced pressure to remove THF and EtOH. The resulting material was diluted with ethyl acetate (50 mL), washed with brine (4 x 50 mL), and water (2 x 50 mL). The combined aqueous fractions were then extracted with chloroform (3 x 50 mL). The combined organic solutions were dried over sodium sulfate, filtered, and concentrated in vacuo to yield 1.56 g of 10-bromoanthracene-9-carbaldehyde oxime (>99%).^{1}H NMR($CDCl_3$) δ 9.22 (s, 1H), 8.51 (s, 1H), 8.42 (d, J=8.66 Hz, 2H), 8.03 (d, J=8.16 Hz, 2H), 7.55 (m, 4H);

To a round bottom flask containing 10-bromoanthracene-9-carbaldehyde oxime (1.05 g, 3.50 mmol) was added chloroform (20 mL) and pyridine (0.350 mmol). To the resulting mixture was added N-bromosuccinimide (0.685 g, 3.85 mmol) portion-wise over 5 minutes. The flask was equipped with a water condenser and the temperature was raised to 40 °C. The resulting turbid mixture was allowed to stir under a balloon of argon for 4 hours. The orange solution with white precipitate was cooled to room temperature and diluted with dichloromethane (150 mL). The resulting solution was washed with brine (3

x 100 mL) and water (2 x 100 mL) before being dried over sodium sulfate. The solution was filtered and concentrated under reduced pressure to yield 1.3 g of the 10-bromo-N-hydroxyanthracene-9-carbimidoyl bromide which can be carried on to the next reaction without further purification.

Under argon, was added ethylacetoacetate (3.10 g, 26.68 mmol) to a solution of sodium ethoxide, prepared by dissolving sodium (0.584 g, 25.4 mmol) in ethanol (100 mL). The resulting solution was then added to a round bottom flask containing 10-bromo-anthracenyl-nitrile oxide (3.8 g, 12.70 mmol). The reaction was allowed to stir at room temperature under argon for 6 hours. The volatiles were removed in vacuo and the resulting brown oil was dissolved in ethyl acetate, washed with brine (4 x 50 mL), and water (4 x 50 mL). The organic layer was then dried over sodium sulfate, filtered, and concentrated to yield 5.2 g of brown solid. The solid was then purified via column chromatography eluting 4:1:1 hexanes: ethylacetate: dichloromethane to yield 4.6 g of orange oil (88 %) which was re-crystallized from $CHCl_3$ and hexanes to yield pure ethyl 3-(anthracen-9-yl)-5-methylisoxazole-4-carboxylate. ^{1}H NMR ($CDCl_3$) δ 8.61 (d, J=8.9 Hz, 2H), 7.61 (m, 4H), 7.46 (m, 2H), 3.71 (q, J=7.1 x (3) Hz, 2H), 2.93 (s, 3H), 0.38 (t, J=7.2 x (2) Hz, 3H)

Fig. 2-2. 3-aryl isoxazole carboxylates

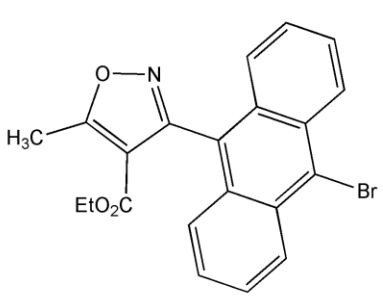

I.

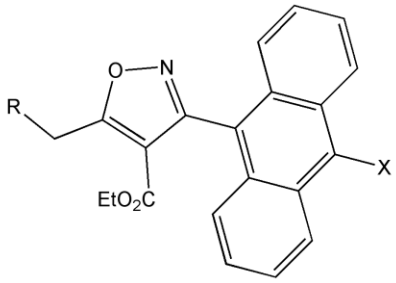

II. R = X = H
III. R = H, X = Cl
IV. R = $PhCH_2$, X=Cl

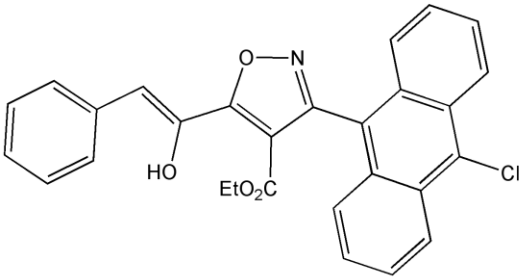

V.

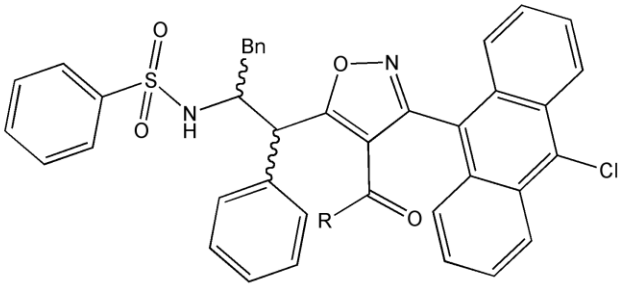

VI. (SR/RS) R = OEt, Bn = $PhCH_2$
VII. (SR/RS) R = n-Bu, Bn = $PhCH_2$

Fig. 2-3. Side view of the title compound

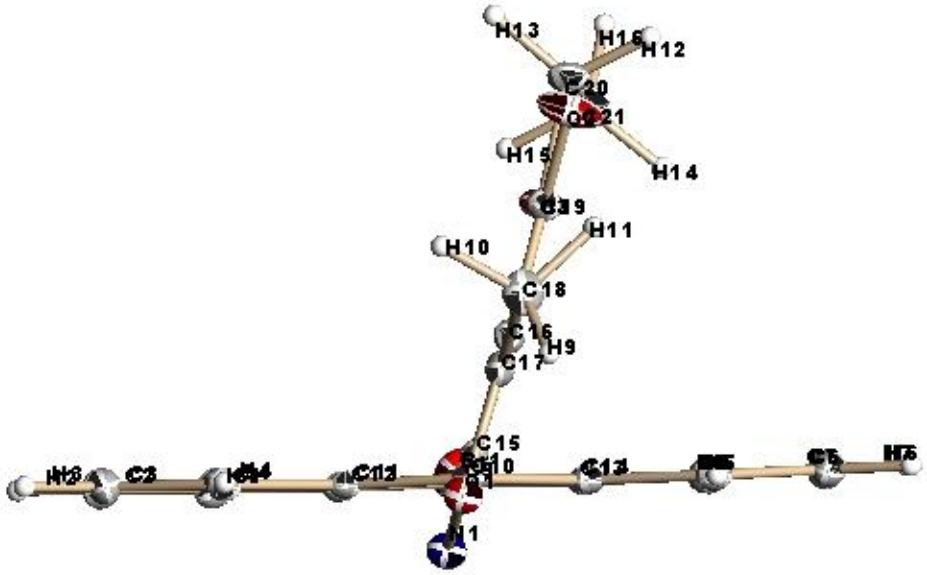

Crystal data

$C_{21}H_{18}BrNO_3$	?
M_r = 412.27	D_x = 1.578 Mg m^{-3}
Monoclinic, $P2_1/c$	Melting point: ? K
Hall symbol: ?	? radiation, λ = 0.71073 Å
a = 8.8554 (4) Å	Cell parameters from 9851 reflections
b = 16.7298 (8) Å	θ = 2.4–28.9°
c = 11.7218 (6) Å	μ = 2.39 mm^{-1}
β = 92.456 (1)°	T = 100 K
V = 1734.98 (14) Å^3	Prism
Z = 4	× × mm
F(000) = 840	

Data collection

? diffractometer	4331 independent reflections
Radiation source: ?	3979 reflections with $I > 2\sigma(I)$

?	R_{int} = 0.020
Detector resolution: 8.3333 pixels mm^{-1}	θ_{max} = 29.0°, θ_{min} = 2.1°
?	h = −11 11
Absorption correction: multi-scan SADABS V2012/1 (Bruker AXS Inc.)	k = −22 22
T_{min} = ?, T_{max} = ?	l = −15 15
20906 measured reflections	

Refinement

Refinement on F^2	Secondary atom site location: difference Fourier map
Least-squares matrix: full	Hydrogen site location: inferred from neighbouring sites
$R[F^2 > 2\sigma(F^2)]$ = 0.028	H atoms treated by a mixture of independent and constrained refinement
$wR(F^2)$ = 0.077	$w = 1/[\sigma^2(F_o^2) + (0.043P)^2 + 1.6812P]$ where $P = (F_o^2 + 2F_c^2)/3$
S = 1.01	$(\Delta/\sigma)_{max}$ = 1.401
4331 reflections	$\Delta\rho_{max}$ = 0.56 e Å^{-3}

237 parameters	$\Delta\rho_{min}$ = −0.35 e Å^{-3}
0 restraints	Extinction correction: none
? constraints	Extinction coefficient: ?
Primary atom site location: structure-invariant direct methods	

Refinement of F^2 against ALL reflections. The weighted R-factor wR and goodness of fit S are based on F^2, conventional R-factors R are based on F, with F set to zero for negative F^2. The threshold expression of $F^2 > 2\text{sigma}(F^2)$ is used only for calculating R-factors(gt) etc. and is not relevant to the choice of reflections for refinement. R-factors based on F^2 are statistically about twice as large as those based on F, and R- factors based on ALL data will be even larger.

Fractional atomic coordinates and isotropic or equivalent isotropic displacement parameters (Å^2)

	x	*y*	*z*	U_{iso}*/U_{eq}
Br1	0.658986 (19)	0.809934 (10)	0.627818 (16)	0.02147 (7)
N1	0.15852 (15)	0.53042 (8)	0.85626 (12)	0.0138 (3)
O1	0.06573 (13)	0.46169 (7)	0.84085 (10)	0.0141 (2)
O2	0.14984 (16)	0.42450 (8)	0.49115 (11)	0.0257 (3)
O3	0.29600 (13)	0.53325 (7)	0.52104 (9)	0.0140 (2)

C1	0.72847 (18)	0.66328 (10)	0.79021 (15)	0.0167 (3)
H1	0.7992	0.703	0.77	0.02*
C2	0.77600 (19)	0.60075 (11)	0.85719 (15)	0.0182 (3)
H2	0.8788	0.5977	0.8834	0.022*
C3	0.67314 (19)	0.54026 (10)	0.88806 (14)	0.0163 (3)
H3	0.7076	0.4969	0.9345	0.02*
C4	0.52499 (18)	0.54413 (10)	0.85133 (13)	0.0136 (3)
H4	0.4575	0.5031	0.8725	0.016*
C5	0.11132 (19)	0.68191 (9)	0.63023 (13)	0.0131 (3)
H5	0.0415	0.6422	0.652	0.016*
C6	0.06338 (19)	0.74251 (10)	0.55974 (14)	0.0164 (3)
H6	−0.0392	0.7444	0.5325	0.02*
C7	0.1655 (2)	0.80264 (10)	0.52684 (15)	0.0180 (3)
H7	0.1308	0.8445	0.4776	0.022*
C8	0.3129 (2)	0.80097 (10)	0.56505 (14)	0.0160 (3)
H8	0.3796	0.8419	0.5423	0.019*
C9	0.52036 (18)	0.73206 (9)	0.67841 (13)	0.0130 (3)

C10	0.31828 (17)	0.61286 (9)	0.73969 (12)	0.0104 (3)
C11	0.46917 (17)	0.60896 (9)	0.78133 (12)	0.0108 (3)
C12	0.57439 (18)	0.67033 (9)	0.74985 (13)	0.0127 (3)
C13	0.36903 (18)	0.73849 (9)	0.63891 (13)	0.0123 (3)
C14	0.26538 (18)	0.67730 (9)	0.67179 (13)	0.0111 (3)
C15	0.21509 (17)	0.54416 (9)	0.75653 (13)	0.0107 (3)
C16	0.16290 (17)	0.48643 (9)	0.67370 (13)	0.0112 (3)
C17	0.07011 (17)	0.43727 (9)	0.73183 (13)	0.0124 (3)
C18	−0.0206 (2)	0.36570 (10)	0.69868 (15)	0.0179 (3)
H9	−0.1069	0.3613	0.7479	0.027*
H10	0.0425	0.3178	0.7073	0.027*
H11	−0.0573	0.3708	0.6189	0.027*
C19	0.19959 (18)	0.47697 (10)	0.55273 (13)	0.0132 (3)
C20	0.34582 (19)	0.52867 (10)	0.40446 (14)	0.0160 (3)
H12	0.258	0.5222	0.3501	0.019*
H13	0.4147	0.4827	0.3959	0.019*
C21	0.4270 (2)	0.60611 (11)	0.38219 (15)	0.0205 (3)

H15	0.5123	0.6122	0.4376	0.031*
H14	0.357	0.651	0.3898	0.031*
H16	0.4644	0.6055	0.3047	0.031*

Atomic displacement parameters (Å^2)

	U^{11}	U^{22}	U^{33}	U^{12}	U^{13}	U^{23}
Br1	0.01677 (10)	0.01705 (10)	0.03110 (11)	−0.00376 (6)	0.00684 (7)	0.00298 (6)
N1	0.0149 (6)	0.0123 (6)	0.0142 (6)	−0.0032 (5)	0.0016 (5)	−0.0003 (5)
O1	0.0150 (5)	0.0135 (5)	0.0138 (5)	−0.0032 (4)	0.0025 (4)	0.0012 (4)
O2	0.0331 (7)	0.0276 (7)	0.0166 (6)	−0.0155 (6)	0.0051 (5)	−0.0083 (5)
O3	0.0171 (6)	0.0145 (5)	0.0107 (5)	−0.0029 (4)	0.0043 (4)	−0.0021 (4)
C1	0.0117 (7)	0.0170 (8)	0.0214 (8)	−0.0015 (6)	0.0008 (6)	−0.0032 (6)
C2	0.0120 (7)	0.0222 (8)	0.0202 (8)	0.0013 (6)	−0.0028 (6)	−0.0048 (7)

C3	0.0171 (8)	0.0179 (8)	0.0136 (7)	0.0038 (6)	−0.0021 (6)	−0.0007 (6)
C4	0.0153 (7)	0.0139 (7)	0.0114 (7)	−0.0002 (6)	0.0001 (5)	−0.0002 (5)
C5	0.0141 (7)	0.0122 (7)	0.0129 (7)	0.0000 (5)	0.0006 (6)	−0.0025 (5)
C6	0.0160 (7)	0.0174 (8)	0.0155 (7)	0.0035 (6)	−0.0018 (6)	−0.0026 (6)
C7	0.0229 (9)	0.0154 (8)	0.0155 (8)	0.0048 (6)	0.0007 (6)	0.0027 (6)
C8	0.0204 (8)	0.0124 (7)	0.0154 (7)	0.0002 (6)	0.0040 (6)	0.0015 (6)
C9	0.0131 (7)	0.0104 (7)	0.0158 (7)	−0.0031 (5)	0.0054 (6)	−0.0014 (6)
C10	0.0116 (7)	0.0105 (7)	0.0092 (6)	−0.0005 (5)	0.0015 (5)	−0.0019 (5)
C11	0.0117 (7)	0.0110 (7)	0.0098 (6)	0.0004 (5)	0.0012 (5)	−0.0022 (5)
C12	0.0120 (7)	0.0129 (7)	0.0135 (7)	−0.0005 (5)	0.0018 (5)	−0.0036 (6)
C13	0.0152 (7)	0.0107 (7)	0.0112 (6)	−0.0001 (5)	0.0026 (5)	−0.0017

						(5)
C14	0.0128 (7)	0.0108 (7)	0.0098 (6)	0.0003 (5)	0.0014 (5)	−0.0022 (5)
C15	0.0105 (7)	0.0100 (7)	0.0116 (7)	0.0017 (5)	0.0000 (5)	0.0009 (5)
C16	0.0104 (6)	0.0113 (7)	0.0118 (7)	−0.0003 (5)	−0.0007 (5)	−0.0003 (5)
C17	0.0113 (7)	0.0121 (7)	0.0138 (7)	0.0016 (5)	−0.0006 (5)	0.0012 (5)
C18	0.0177 (8)	0.0131 (7)	0.0226 (8)	−0.0043 (6)	−0.0016 (6)	0.0017 (6)
C19	0.0129 (7)	0.0141 (7)	0.0126 (7)	−0.0001 (6)	0.0004 (5)	−0.0007 (6)
C20	0.0202 (8)	0.0177 (8)	0.0105 (7)	0.0009 (6)	0.0048 (6)	−0.0006 (6)
C21	0.0234 (9)	0.0214 (8)	0.0173 (8)	−0.0023 (7)	0.0063 (6)	0.0026 (6)

Geometric parameters (Å, °)

Br1—C9	1.9022 (15)	C8—C13	1.433 (2)
N1—C15	1.312 (2)	C8—H8	0.95

N1—O1	1.4203 (17)	C9—C12	1.401 (2)
O1—C17	1.3438 (19)	C9—C13	1.403 (2)
O2—C19	1.208 (2)	C10—C11	1.404 (2)
O3—C19	1.3344 (19)	C10—C14	1.408 (2)
O3—C20	1.4558 (18)	C10—C15	1.487 (2)
C1—C2	1.364 (2)	C11—C12	1.445 (2)
C1—C12	1.430 (2)	C13—C14	1.439 (2)
C1—H1	0.95	C15—C16	1.432 (2)
C2—C3	1.419 (2)	C16—C17	1.365 (2)
C2—H2	0.95	C16—C19	1.477 (2)
C3—C4	1.365 (2)	C17—C18	1.484 (2)
C3—H3	0.95	C18—H9	0.98
C4—C11	1.435 (2)	C18—H10	0.98
C4—H4	0.95	C18—H11	0.98
C5—C6	1.364 (2)	C20—C21	1.510 (2)
C5—C14	1.431 (2)	C20—H12	0.99
C5—H5	0.95	C20—H13	0.99

C6—C7	1.417 (2)	C21—H15	0.98
C6—H6	0.95	C21—H14	0.98
C7—C8	1.362 (3)	C21—H16	0.98
C7—H7	0.95		
C15—N1—O1	105.64 (12)	C1—C12—C11	118.26 (15)
C17—O1—N1	109.08 (12)	C9—C13—C8	123.85 (14)
C19—O3—C20	116.58 (12)	C9—C13—C14	117.93 (14)
C2—C1—C12	121.36 (16)	C8—C13—C14	118.19 (15)
C2—C1—H1	119.3	C10—C14—C5	121.52 (14)
C12—C1—H1	119.3	C10—C14—C13	119.71 (14)
C1—C2—C3	120.55 (15)	C5—C14—C13	118.71 (14)
C1—C2—H2	119.7	N1—C15—C16	111.20 (14)
C3—C2—H2	119.7	N1—C15—C10	120.94 (13)
C4—C3—C2	120.31 (15)	C16—C15—C10	127.86 (14)
C4—C3—H3	119.8	C17—C16—C15	104.56 (13)
C2—C3—H3	119.9	C17—C16—C19	125.22 (14)
C3—C4—C11	121.28 (15)	C15—C16—C19	130.20 (14)

C3—C4—H4	119.4	O1—C17—C16	109.51 (13)
C11—C4—H4	119.4	O1—C17—C18	117.19 (14)
C6—C5—C14	120.91 (15)	C16—C17—C18	133.30 (15)
C6—C5—H5	119.5	C17—C18—H9	109.5
C14—C5—H5	119.6	C17—C18—H10	109.5
C5—C6—C7	120.45 (15)	H9—C18—H10	109.5
C5—C6—H6	119.8	C17—C18—H11	109.5
C7—C6—H6	119.8	H9—C18—H11	109.5
C8—C7—C6	120.65 (15)	H10—C18—H11	109.5
C8—C7—H7	119.7	O2—C19—O3	124.60 (15)
C6—C7—H7	119.7	O2—C19—C16	124.20 (15)
C7—C8—C13	121.09 (15)	O3—C19—C16	111.19 (13)
C7—C8—H8	119.4	O3—C20—C21	106.43 (13)
C13—C8—H8	119.5	O3—C20—H12	110.4
C12—C9—C13	123.42 (14)	C21—C20—H12	110.4
C12—C9—Br1	118.87 (12)	O3—C20—H13	110.5
C13—C9—Br1	117.68 (12)	C21—C20—H13	110.5

C11—C10—C14	121.37 (14)	H12—C20—H13	108.6
C11—C10—C15	119.94 (13)	C20—C21—H15	109.4
C14—C10—C15	118.38 (13)	C20—C21—H14	109.5
C10—C11—C4	122.22 (14)	H15—C21—H14	109.5
C10—C11—C12	119.51 (14)	C20—C21—H16	109.5
C4—C11—C12	118.23 (14)	H15—C21—H16	109.5
C9—C12—C1	123.73 (15)	H14—C21—H16	109.5
C9—C12—C11	117.97 (14)		

Torsion Angles

C15—N1—O1—C17	−0.30 (16)	C11—C10—C14—C13	3.4 (2)
C12—C1—C2—C3	0.5 (3)	C15—C10—C14—C13	−170.20 (13)
C1—C2—C3—C4	−0.2 (3)	C6—C5—C14—C10	−176.61 (15)
C2—C3—C4—C11	−0.2 (2)	C6—C5—C14—C13	0.7 (2)
C14—C5—C6—C7	−0.4 (2)	C9—C13—C14—C10	−1.2 (2)
C5—C6—C7—C8	−0.1 (3)	C8—C13—C14—C10	176.87 (14)
C6—C7—C8—C13	0.3 (3)	C9—C13—C14—C5	−178.62 (14)
C14—C10—C11—C4	179.52 (14)	C8—C13—C14—C5	−0.5 (2)

C15—C10—C11—C4	−7.0 (2)	O1—N1—C15—C16	0.03 (17)
C14—C10—C11—C12	−2.8 (2)	O1—N1—C15—C10	179.54 (12)
C15—C10—C11—C12	170.64 (13)	C11—C10—C15—N1	75.95 (19)
C3—C4—C11—C10	177.99 (15)	C14—C10—C15—N1	−110.38 (17)
C3—C4—C11—C12	0.3 (2)	C11—C10—C15—C16	−104.62 (18)
C13—C9—C12—C1	179.85 (15)	C14—C10—C15—C16	69.0 (2)
Br1—C9—C12—C1	1.8 (2)	N1—C15—C16—C17	0.23 (18)
C13—C9—C12—C11	2.0 (2)	C10—C15—C16—C17	−179.24 (14)
Br1—C9—C12—C11	−176.09 (11)	N1—C15—C16—C19	−178.08 (15)
C2—C1—C12—C9	−178.22 (16)	C10—C15—C16—C19	2.4 (3)
C2—C1—C12—C11	−0.3 (2)	N1—O1—C17—C16	0.45 (17)
C10—C11—C12—C9	0.2 (2)	N1—O1—C17—C18	−179.92 (13)
C4—C11—C12—C9	177.94 (14)	C15—C16—C17—O1	−0.42 (17)
C10—C11—C12—C1	−177.81 (14)	C19—C16—C17—O1	178.01 (14)
C4—C11—C12—C1	−0.1 (2)	C15—C16—C17—C18	−179.96 (17)
C12—C9—C13—C8	−179.42 (15)	C19—C16—C17—C18	−1.5 (3)
Br1—C9—C13—C8	−1.4 (2)	C20—O3—C19—O2	−1.5 (2)

C12—C9—C13—C14	−1.4 (2)	C20—O3—C19—C16	177.71 (13)
Br1—C9—C13—C14	176.63 (11)	C17—C16—C19—O2	0.7 (3)
C7—C8—C13—C9	178.02 (16)	C15—C16—C19—O2	178.68 (17)
C7—C8—C13—C14	0.0 (2)	C17—C16—C19—O3	−178.56 (14)
C11—C10—C14—C5	−179.32 (14)	C15—C16—C19—O3	−0.6 (2)
C15—C10—C14—C5	7.1 (2)	C19—O3—C20—C21	169.02 (14)

All esds (except the esd in the dihedral angle between two l.s. planes) are estimated using the full covariance matrix. The cell esds are taken into account individually in the estimation of esds in distances, angles and torsion angles; correlations between esds in cell parameters are only used when they are defined by crystal symmetry. An approximate (isotropic) treatment of cell esds is used for estimating esds involving l.s. planes.

Chapter 3: Future Work

As our approach is hypothesis-driven structure based rational drug design, my continuing contribution to the AIMs project is to include both mechanistic and synthetic studies. In order to advance our understanding of the mechanism by which the AIMs exhibit their anti-tumor activity I intend to determine the ability of our lead compounds to interact with G4 derived from telomeric, oncogenic, and mitochondrial DNA. This data will facilitate determination of key interactions that will allow for the design of sequence specific quadruplex binding molecules.

One method by which we propose to amplify selectivity and inherently efficacy is to introduce axial chirality into the AIMs. It is often true that diasteriomers exhibit different selectivity and affinity for a given target; the introduction of axial chirality into the AIMs will allow for the exploitation of this fact. Currently we are exploring both intramolecular lateral metalations and unsymmetrical halogenations. This work will be completed in route to a Ph.D. Progress will be reported in due course.